CHINESE OPTICS LETTERS

Vol. 20, No. 10 | October 2022

# Photoinduced excimer generation in perylene diimide dimer: effects of solvent polarity [Invited]

Guangliu Ran (冉光柳)[1], Hang Wang (汪 航)[2], Yujing Song (宋宇菁)[1], Yahui Liu (刘亚辉)[2], Zhishan Bo (薄志山)[2,3], and Wenkai Zhang (张文凯)[1*]

[1] Department of Physics and Applied Optics Beijing Area Major Laboratory, Center for Advanced Quantum Studies, Beijing Normal University, Beijing 100875, China

[2] College of Textiles & Clothing, Qingdao University, Qingdao 266071, China

[3] Beijing Key Laboratory of Energy Conversion and Storage Materials, College of Chemistry, Beijing Normal University, Beijing 100875, China

*Corresponding author: wkzhang@bnu.edu.cn

Received August 16, 2022 | Accepted September 8, 2022 | Posted Online October 8, 2022

The aggregation and photoinduced excited state dynamics of organic $\pi$-conjugated molecules play a vital role in solar energy conversion and applications. This work investigates how solvent polarity affects the aggregation behavior and the photophysical process of perylene diimide dimer (PDI-II). The results show that the conjugations between PDI intramolecular chromophores are more likely to generate excimer, and the conjugations between PDI intermolecular chromophores are more likely to experience symmetry-breaking charge separation. Our study can provide a reference for the design of high-efficiency solar energy conversion materials.

**Keywords:** excimer; perylene diimide; dimer; solvent effect; transient absorption spectroscopy.
**DOI:** 10.3788/COL202220.100009

## 1. Introduction

Functional organic materials play a vital role in solar energy conversion and applications. The organic $\pi$-conjugated molecules are the most used functional organic materials, which mainly refer to molecules containing many benzene rings, such as boron dipyrromethene, porphyrin, perylene, and perylene diimide (PDI)[1]. These organic $\pi$-conjugated molecules have been widely used in photovoltaics, photosynthesis, photoelectricity, photocatalysis, etc.[2–7]. Understanding the microscopic dynamic behavior of organic $\pi$-conjugated molecules is crucial for further understanding the photophysical processes to help better applications[8,9]. Previous studies have shown that this conjugate molecule has many complex and exciting dynamic processes, such as excimer state, singlet fission (SF), and symmetry-breaking charge separation (SB-CS)[10–12]. Various structures and complex dynamics interest researchers. The excimer state is often considered a mixture of locally excited (LE) state and charge transport (CT) state, which belongs to a trap state[13,14]. However, in some studies, excimer is also believed to be beneficial to charge separation and SF[15]. SF is a process in which a singlet state splits into two triplet states. In organic photovoltaics, singlet splitting is generally considered to increase the theoretical limit of organic photovoltaics beyond the Shockley–Queisser limit[16]. The SB-CS process refers to forming radical cations and anions in $\pi$-conjugated molecules after photoexcitation, which is conducive to charge separation.

PDI is a typical organic $\pi$-conjugated molecule, applied in many fields due to its diverse structure and abundant dynamic processes. Our group previously reported on the aggregation behavior of PDI monomers under hydrophobic effect and the SB-CS process after aggregation[11]. Here, we used the identical PDI monomers (PDI-C5) as the basic unit to synthesize a dimer molecule (PDI-II), whose structure is shown in Fig. 1. This work studied PDI-II's aggregation behavior and dynamics in different solvents. Unlike the aggregation of PDI-C5, we find excimer formation instead of SB-CS when PDI-II is dissolved in the high polarity solvent. This finding is of great significance. Since the generation of SB-CS and excimer states is inseparable from electronic coupling, we suspect that the difference in products is because the aggregation of PDI-C5 in solution belongs to intermolecular aggregation. The electronic coupling between PDI-C5 chromophores is weak. However, when the two chromophores are connected by conjugated bridge structures and are in a highly polar solvent, the electronic coupling is further enhanced, and excimer is formed. Our study demonstrates that the excited state dynamics of molecules can be controlled by molecular design and solvation.

## 2. Experimental and Methods

### 2.1. Synthesis

The details of molecular structures, design, and synthesis methods of PDI-II can be seen in the literature[17]. All the essential materials and organic solvents were bought from certified commercial resources and used as received.

### 2.2. Steady-state and femtosecond transient absorption spectroscopy

For solution experiments, ultraviolet–visible (UV–Vis), and fluorescence, and femtosecond transient absorption (Fs-TA) spectra were recorded with Agilent Technologies Cary 60 UV–Vis spectrophotometer, FLS980 spectrometer (Edinburgh), and Fs-TA spectrometer (Harpia-TA, Light Conversion), respectively. Details of the instrument have been described in a previous article[18]. The Fs-TA experiment was done several times on different spots of the sample, and when measurement was completed, no sample degradation was detected. For UV–Vis and Fs-TA, the concentration was $10^{-5}$ mol/L; for fluorescence, the concentration was $10^{-6}$ mol/L. The fluorescence quantum yield was measured by the comparative method of Williams *et al.*[19], and the yield of Rhodamine 6G in ethanol was taken as the standard yield.

## 3. Results and Discussion

The PDI-C5's molecular structure is shown in Fig. 1(a). The molecule contains two aliphatic branches or "swallow-tail" side chains in the imide position, improving the solubility[20]. The molecular structure of PDI-II is shown in Fig. 1(b). We modify the bay position of the PDI-C5 and then connect the two PDI-C5s to the central benzene core by an acetylene spacer to form a dimer (PDI-II)[17]. The flexibility of the alkyne bond makes it possible for the solvent to regulate the strength of the electronic coupling between the two chromophores. The absorption and fluorescence spectra of PDI-C5 in dichloromethane (DCM), tetrahydrofuran (THF), and acetone are shown in Fig. 1(c). As shown in Fig. 1(c), PDI-C5 shows three absorption peaks with apparent fine structure in solution, corresponding to the vibrational transition of $S_0 - S_1$ [21]. The vibrational transition intensity progression follows the order $A_{0-0}$(502–550 nm) > $A_{0-1}$(460–502 nm) > $A_{0-2}$(435–466 nm), which are the PDI monomer absorption characteristics[22]. At the same time, with increasing solvent polarity, the profile of the absorption spectrum remains consistent. Still, it appears to have a slight blueshift because of different energy levels of the excited states of the perylene moieties[23]. The fluorescence spectrum of PDI-C5 showed a mirror image symmetric configuration with the absorption spectrum, proving that PDI-C5 has a monomeric feature in these three solvents[24]. The absorption and fluorescence spectra of PDI-II in the three solvents are shown in Fig. 1(d). PDI-II showed three characteristic absorption peaks with prominent fine structures in DCM and THF and followed the order $A_{0-0}$(527–595 nm) > $A_{0-1}$(488–527 nm) > $A_{0-2}$(440–488 nm). Different from Fig. 1(c), the three absorption peaks are redshifted and broader, which is caused by the link of the conjugated bridge structure and increases the electronic coupling of the PDI-II chromophore[25]. The absorption spectrum of PDI-II in acetone appears strange, possibly due to the aggregation of PDI-II in highly polar solvents[22,26]. The fluorescence spectra in Fig. 1(d) become broader and less structured. Especially for PDI-II in acetone, the 650–750 nm fluorescence becomes obvious, indicating the excimer formation[27]. We measured the fluorescence lifetime ($\tau$) and corresponding fluorescence quantum yield ($\Phi$) in solution; the results are shown in Table 1. With increasing solvent polarity, the lifetime of both molecules changes slightly. However, the PDI-II's quantum yield decreases sharply with increasing solvent polarity and is almost quenched in the highly polar solvent. This phenomenon implies that PDI-II relaxes to a nonradiative state in high-polarity solvents[25,28].

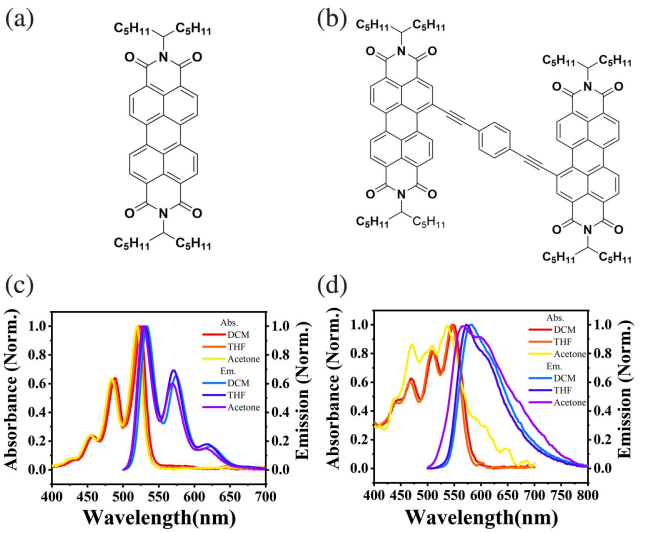


**Fig. 1.** (a) Molecular structure of PDI-C5; (b) molecular structure of PDI-II; (c) normalized absorption and fluorescence spectra of PDI-C5 in solvents; (d) normalized absorption and fluorescence spectra of PDI- II in solvents.

**Table 1.** Fluorescence Quantum Yields and Corresponding Fluorescence Lifetime of PDI-C5 and PDI-II in Different Solvents.

| Molecule | Solution | Polarity | $\Phi$ | $\tau$ (ns) |
|---|---|---|---|---|
| PDI-C5 | DCM | 3.4 | > 0.95 | 4.29 |
| | THF | 4.2 | > 0.95 | 4.17 |
| | Acetone | 5.4 | > 0.95 | 4.31 |
| PDI- II | DCM | 3.4 | 0.61 | 5.43 |
| | THF | 4.2 | 0.27 | 5.24 |
| | Acetone | 5.4 | 0.04 | 5.79 |

Fs-TA spectroscopy was used to study PDI-II molecular excited-state energy transfer mechanism in solutions. For comparison, the excited-state dynamics process of PDI-C5 is measured and shown in Fig. 2. As shown in Figs. 2(a)–2(c), three consecutive negative peaks and a broad positive signal appear. Compared with the absorption and fluorescence spectrum label in the figures, we conclude that the negative peak is near 530, 620 nm is the stimulated radiation (SE), and the sharp and high-intensity signal at 500–550 nm belongs to the superposition of the ground state bleaching (GSB) and SE. This mountain-like signal is in good agreement with the absorption and fluorescence spectra and is consistent with the high fluorescence quantum yield of PDI-C5 in the three solvents (Table 1). The sharp positive signal between 670 and 760 nm belongs to the LE state or excited singlet state[29]. After photoexcitation, the positive signal in the 630–910 nm range appeared and increased together with the GSB signal. According to the literature, this prolonged signal growth is caused by vibrational relaxation of the hot singlet state or the charge transfer (CT) process[25]. By comparing the various dynamic processes in Fig. 2, PDI-C5 showed almost the same dynamics process in the three solvents, which means that the solvent polarity has little influence on the dynamics process of simple PDI monomer molecules.

Figure 3 shows the excited-state dynamics process of PDI-II in three solvents, and the TA results under different solvents have apparent differences. Figure 3(a) shows the dynamics process of PDI-II in DCM. The results are the same as in Fig. 2. Compared with the absorption and fluorescence spectra, the negative peak at 500 nm is GSB, the peak at 600 nm is SE, and the middle high-intensity peak is the superposition signal of GSB and SE. The positive signal in the 610–910 nm band appeared and increased together with the GSB, the same as the PDI-C5, caused by the vibrational relaxation of the hot singlet state[25]. Figures 3(b) and 3(e) show the TA spectra of PDI-II in THF. Unlike Fig. 3(a), a clear positive signal appears in the 580–720 nm range and forms an isosbestic point at 712 nm. It has been reported that the excimer state has a strong characteristic absorption signal in the 600–800 nm band[16,30]. The excimer state usually appears as a trap state, leading to fluorescence quenching[15,31]. We attribute this new absorption signal to the excimer. In some studies, the excimer is also believed beneficial to charge separation and SF[15,32]. Since no new positive signal emerges in the range of 750–910 nm, which is the absorption range of PDI radical anions[10–12,25,32], we exclude the generation of the SB-CS process. Since the fluorescence did not appear to have a long lifetime, we excluded the SF process. Figure 3(c) and 3(f) show the dynamic process of PDI-II in acetone. PDI-II shows a different dynamic process in acetone than in the previous two solvents. In Fig. 3(c), there is only one wide negative signal generation. The one negative peak is attributed to the PDI-II aggregates in acetone, leading to enhanced conjugation, so the absorption spectrum is concentrated near

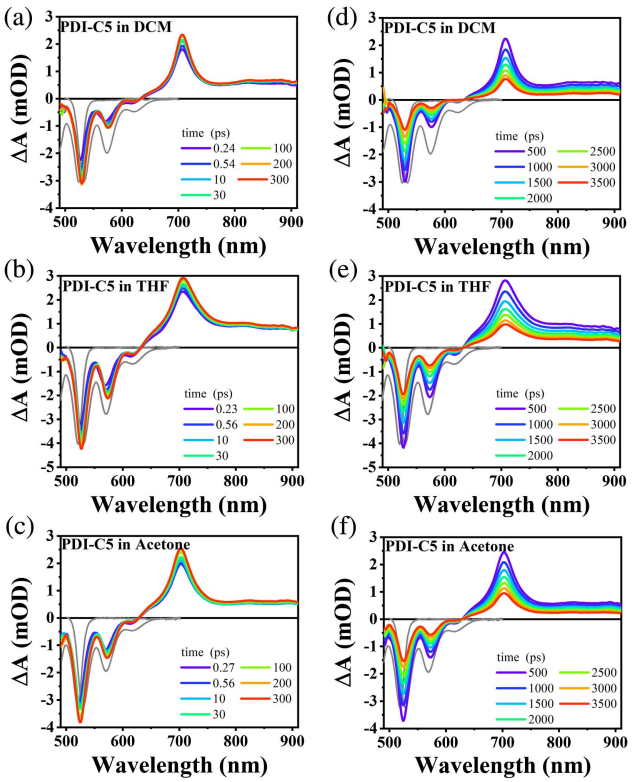


**Fig. 2.** TA spectra at selected delay time of PDI-C5 in (a), (d) DCM, (b), (e) THF, and (c), (f) acetone. (a)–(c) show short time decay range. (d)–(f) show long time decay range. Excited at 480 nm.

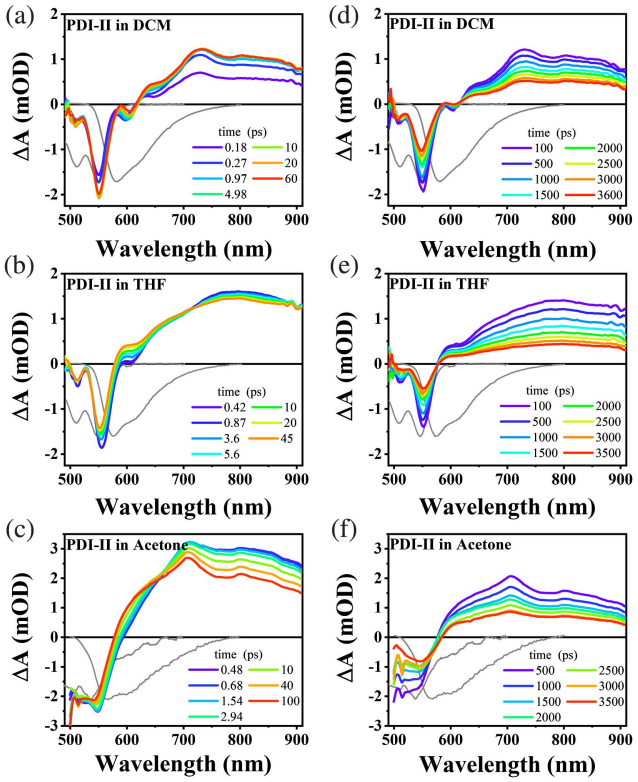


**Fig. 3.** TA spectra at selected delay time of PDI-II in (a), (d) DCM, (b), (e) THF, and (c), (f) acetone. (a)–(c) show short time decay range. (d)–(f) show long time decay range. Excited at 480 nm.

550 nm, and fluorescence quenching simultaneously causes the SE signal around 600 nm to almost disappear. The positive signal at 0.5 ps is the same as in Fig. 3(a), ascribed to the LE. But a new positive peak in the 578–668 nm range is the same as in Fig. 3(b) and can be ascribed to the excimer.

Combined with the above analysis, the global fitting can well decompose the various excited state components and the corresponding decay time during the decay process. For PDI-C5 in the three solvents and PDI-II in DCM, two continuous processes provide an excellent fit for the dynamic process. However, for PDI-II in THF and acetone, three components are needed to fit the kinetic process because of the generation of the excimer. The species-associated difference spectra (SADSs) and corresponding concentrations are shown in Figs. 4 and 5. The time constants of corresponding excited-state processes are presented in Table 2. The global fitting results of PDI-C5 in the three solvents are shown in Fig. 4. PDI-C5 presents the same dynamics process in the three solvents; this coincides with the above discussion that PDI-C5 is a monomer state in these solvents. The 480 nm high-energy photon excites the PDI-C5 to the high vibrational level of the lowest singly excited state (LE state) and then undergoes a vibrational relaxation process (~120 ps) to the lowest vibrational $S_1$ (or CT). The second time constants (~3 ns) are attributed to the relaxed $S_1$ back to the ground state.

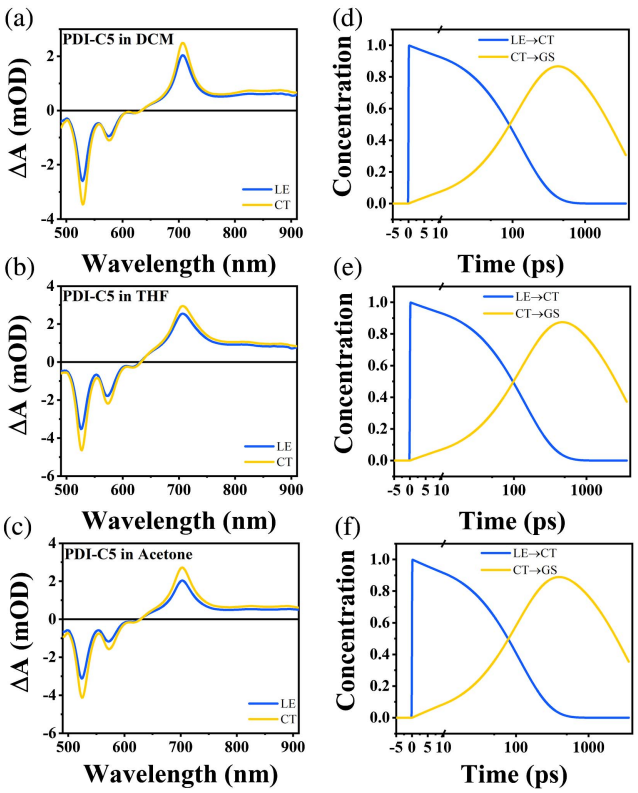


**Fig. 4.** Global target analysis results derived from Fs-TA of PDI-C5. SADSs and population of PDI-C5 in (a), (d) DCM, (b), (e) THF, and (c), (f) acetone (LE is locally excited, CT is charge transfer, and GS is ground state).

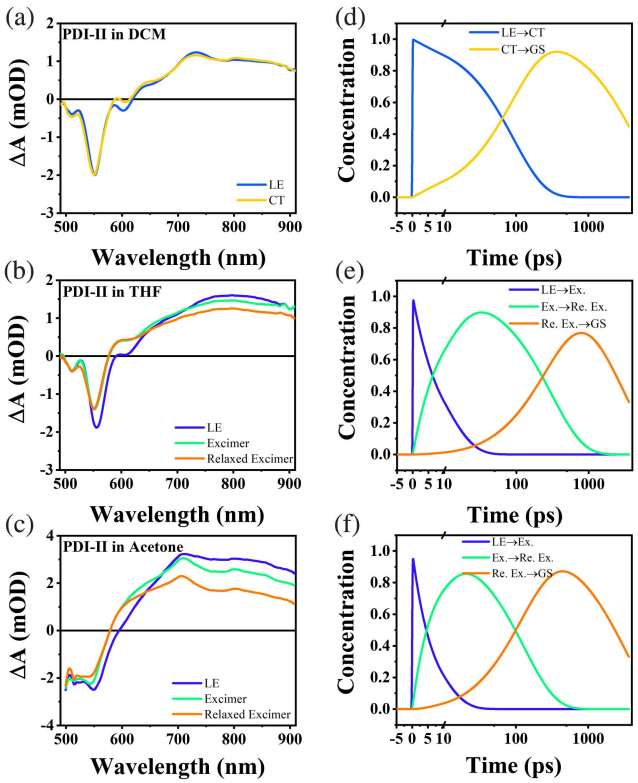


**Fig. 5.** Global target analysis results derived from Fs-TA of PDI-II. SADSs and population of PDI-II in (a), (d) DCM, (b), (e) THF, and (c), (f) acetone (Ex. is excimer; Re. Ex. is relaxed excimer).

**Table 2.** Time Constants Estimated for Different Processes of PDI-C5 and PDI-II in Different Solvents Determined by Fs-TA Measurements.

| Molecular | Solution | $\tau_1$ (ps) | $\tau_2$ (ps) | $\tau_3$ (ps) | $\tau_4$ (ps) |
|---|---|---|---|---|---|
| PDI-C5 | DCM | 129 ± 1 | 2957 ± 11 | – | – |
| | THF | 139 ± 1 | 3417 ± 14 | – | – |
| | Acetone | 113 ± 6 | 3335 ± 31 | – | – |
| PDI-II | DCM | 92 ± 17 | 4402 ± 54 | – | |
| | THF | 7.69 ± 0.71 | – | 213 ± 76 | 2874 ± 56 |
| | Acetone | 6.48 ± 0.72 | – | 131 ± 25 | 3169 ± 117 |

Figure 5 shows the global fitting results of PDI-II in the three solvents. Since PDI-II exhibits monomer characteristics in DCM, two components are sufficient for fitting; the result is shown in Figs. 5(a) and 5(d). The results are almost consistent with the PDI-C5, which consists of a fast vibrational relaxation process (~90 ps) and a slow recombination process (~4 ns). However, for PDI-II in THF and acetone, the generation of excimer states makes them present different dynamics processes. The second and third SADSs in Figs. 5(b) and 5(c) show a

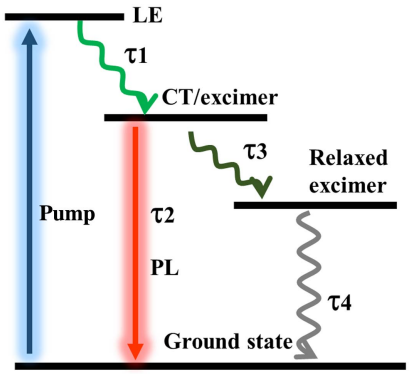


**Fig. 6.** Jablonski diagram illustrating the kinetic model used to fit TA from PDI-C5 and PDI-II solutions.

new absorption peak around 578–720 nm is consistent with the previous analysis. According to the above study, a simple fitted model diagram can illustrate various kinetic processes of PDI-II in solution (Fig. 6). For PDI-II in DCM, LE states are generated immediately after photoexcitation, undergo a vibrational relaxation, and return to the ground state through a radiative relaxation process. But due to high polarity interaction enhanced electronic coupling, the excimer states are generated in THF and acetone, then come across a structural relaxation, and return to the ground state.

## 4. Conclusion

We have studied a PDI dimer's steady-state spectral characteristics and excited state dynamics under different solvents. Steady-state spectral results show that the UV–Vis spectra show aggregation characteristics with increasing solvent polarity while the fluorescence quantum yield decreases. Transient absorption spectra show that the excited state energy relaxes to the ground state by excimer in a highly polar solvent. Previous studies have shown that when monomer PDI-C5 aggregates under the hydrophobicity effect, it finally produces the SB-CS. However, in this work, we found that the aggregation of dimers under the solvent polarity effect will form the excimer. Since the excimer and SB-CS are closely related to the electronic coupling between the chromophores, we believe that this product gap is caused by the conjugated bridge structure in the middle of the dimer, which enhances the electronic coupling. We demonstrated that excimer formation was achieved in dimer molecules through molecular design and solvent regulation. Our research can provide a reference for the design of high-efficiency solar energy conversion materials.

## Acknowledgement

This work was supported by the National Natural Science Foundation of China (No. U2032112).

## References

1. N. A. Bumagina, E. V. Antina, A. A. Ksenofontov, L. A. Antina, A. A. Kalyagin, and M. B. Berezin, "Basic structural modifications for improving the practical properties of BODIPY," Coord. Chem. Rev. **469**, 214684 (2022).
2. S. Silvestri, A. R. Fajardo, and B. A. Iglesias, "Supported porphyrins for the photocatalytic degradation of organic contaminants in water: a review," Environ. Chem. Lett. **20**, 731 (2022).
3. P. Murugan, T. Hu, X. Hu, and Y. Chen, "Advancements in organic small molecule hole-transporting materials for perovskite solar cells: past and future," J. Mater. Chem. A **10**, 5044 (2022).
4. A. K. Mitra, "Sesquicentennial birth anniversary of carbazole, a multifaceted wonder molecule: a revisit to its synthesis, photophysical and biological studies," J. Iran. Chem. Soc. **19**, 2075 (2022).
5. M. Ciganek, J. Richtar, M. Weiter, and J. Krajcovic, "Organic π-conjugated molecules: from nature to artificial applications. where are the boundaries?" Isr. J. Chem. **62**, e202100061 (2022).
6. D. Barman, K. Narang, R. Parui, N. Zehra, M. N. Khatun, L. R. Adil, and P. K. Iyer, "Review on recent trends and prospects in π-conjugated luminescent aggregates for biomedical applications," Aggregate, e172 (2022).
7. L. Luo, W. Huang, C. Yang, J. Zhang, and Q. Zhang, "Recent advances on pi-conjugated polymers as active elements in high performance organic field-effect transistors," Front. Phys. **16**, 33500 (2021).
8. Y. Hino, T. Matsuo, and S. Hayashi, "Structural phase transitions in anthracene crystals," Chempluschem **87**, e202200157 (2022).
9. L. Zhang, Z. Chen, F. Sun, Y. Wang, H. Bao, X. Gao, and Z. Liu, "Progress of monomeric perylene diimide derivatives as non-fullerene acceptors for organic solar cells," J. Electron. Mater. **51**, 4224 (2022).
10. C. Lin, T. Kim, J. D. Schultz, R. M. Young, and M. R. Wasielewski, "Accelerating symmetry-breaking charge separation in a perylenediimide trimer through a vibronically coherent dimer intermediate," Nat. Chem. **14**, 786 (2022).
11. G. Ran, J. Zeb, Y. Song, P. A. Denis, U. Ghani, and W. Zhang, "Photoinduced symmetry breaking-charge separation in the aggregated state of perylene diimide: effect of hydrophobicity," J. Phys. Chem. C **126**, 3872 (2022).
12. E. Sebastian and M. Hariharan, "Symmetry-breaking charge separation in molecular constructs for efficient light energy conversion," ACS Energy Lett. **7**, 696 (2022).
13. M. Son, K. H. Park, C. Shao, F. Wuerthner, and D. Kim, "Spectroscopic demonstration of exciton dynamics and excimer formation in a sterically controlled perylene bisimide dimer aggregate," J. Phys. Chem. Lett. **5**, 3601 (2014).
14. K. E. Brown, W. A. Salamant, L. E. Shoer, R. M. Young, and M. R. Wasielewski, "Direct observation of ultrafast excimer formation in covalent perylenediimide dimers using near-infrared transient absorption spectroscopy," J. Phys. Chem. Lett. **5**, 2588 (2014).
15. W. Kim, A. Nowak-Krol, Y. Hong, F. Schlosser, F. Wuerthner, and D. Kim, "Solvent-modulated charge-transfer resonance enhancement in the excimer state of a bay-substituted perylene bisimide cyclophane," J. Phys. Chem. Lett. **10**, 1919 (2019).
16. Y. Hong, J. Kim, W. Kim, C. Kaufmann, H. Kim, F. Wuerthner, and D. Kim, "Efficient multiexciton state generation in charge-transfer-coupled perylene bisimide dimers via structural control," J. Am. Chem. Soc. **142**, 7845 (2020).
17. H. Wang, M. Li, Y. Liu, J. Song, C. Li, and Z. Bo, "Perylene diimide based star-shaped small molecular acceptors for high efficiency organic solar cells," J. Mater. Chem. C **7**, 819 (2019).
18. G. Ran, J. Zeb, H. Lu, Y. Liu, A. Zhang, L. Wang, Z. Bo, and W. Zhang, "Ultrafast carrier dynamics of non-fullerene acceptors with different planarity: impact of steric hindrance," J. Phys. Chem. Lett. **13**, 5860 (2022).
19. A. T. R. Williams, S. A. Winfield, and J. N. Miller, "Relative fluorescence quantum yields using a computer-controlled luminescence spectrometer," Analyst **108**, 1067 (1983).
20. X. Xu, A. Austin, S. E. Mylon, J. Plenge, and J. M. Szarko, "Improving the quantum yields of perylene diimide aggregates by increasing molecular hydrophobicity in polar media," ChemPhysChem **18**, 2430 (2017).
21. S. Kang, T. Kim, Y. Hong, F. Wuerthner, and D. Kim, "Charge-delocalized state and coherent vibrational dynamics in rigid PBI H-aggregates," J. Am. Chem. Soc. **143**, 9825 (2021).

22. Z. Chen, B. Fimmel, and F. Wuerthner, "Solvent and substituent effects on aggregation constants of perylene bisimide π-stacks: a linear free energy relationship analysis," Org. Biomol. Chem. **10**, 5845 (2012).
23. M. R. Islam and P. R. Sundararajan, "Self-assembly of a set of hydrophilic-solvophobic-hydrophobic coil-rod-coil molecules based on perylene diimide," Phys. Chem. Chem. Phys. **15**, 21058 (2013).
24. C. Kaufmann, W. Kim, A. Nowak-Krol, Y. Hong, D. Kim, and F. Wuerthner, "Ultrafast exciton delocalization, localization, and excimer formation dynamics in a highly defined perylene bisimide quadruple pi-stack," J. Am. Chem. Soc. **140**, 4253 (2018).
25. J. Kong, W. Zhang, G. Li, D. Huo, Y. Guo, X. Niu, Y. Wan, B. Tang, and A. Xia, "Excited-state symmetry-breaking charge separation dynamics in multi-branched perylene diimide molecules," J. Phys. Chem. Lett. **11**, 10329 (2020).
26. F. Wuerthner, "Solvent effects in supramolecular chemistry: linear free energy relationships for common intermolecular interactions," J. Org. Chem. **87**, 1602 (2022).
27. J. Sung, P. Kim, B. Fimmel, F. Wuerthner, and D. Kim, "Direct observation of ultrafast coherent exciton dynamics in helical pi-stacks of self-assembled perylene bisimides," Nat. Commun. **6**, 8646 (2015).
28. I. Solymosi, S. Krishna, E. Nuin, H. Maid, B. Scholz, D. M. Guldi, M. E. Perez-Ojeda, and A. Hirsch, "Diastereoselective formation of homochiral flexible perylene bisimide cyclophanes and their hybrids with fullerenes," Chem. Sci. **12**, 15491 (2021).
29. Y. Y. Guo, Z. T. Ma, X. M. Niu, W. Zhang, M. Tao, Q. J. Guo, Z. H. Wang, and A. D. Xia, "Bridge-mediated charge separation in isomeric N-annulated perylene diimide dimers," J. Am. Chem. Soc. **141**, 12789 (2019).
30. J. Sung, A. Nowak-Krol, F. Schlosser, B. Fimmel, W. Kim, D. Kim, and F. Wuerthner, "Direct observation of excimer-mediated intramolecular electron transfer in a cofacially-stacked perylene bisimide pair," J. Am. Chem. Soc. **138**, 9029 (2016).
31. E. Sebastian and M. Hariharan, "Null exciton-coupled chromophoric dimer exhibits symmetry-breaking charge separation," J. Am. Chem. Soc. **143**, 13769 (2021).
32. C. E. Ramirez, S. Chen, N. E. Powers-Riggs, I. Schlesinger, R. M. Young, and M. R. Wasielewski, "Symmetry-breaking charge separation in the solid state: tetra(phenoxy)perylenediimide polycrystalline films," J. Am. Chem. Soc. **142**, 18243 (2020).